

Electronic Supplementary Information

for: Sorting droplets into many outlets

Saurabh Vyawahare,^{*a} Michael Brundage,^a Aleksandra Kijac,^a Michael Gutierrez,^a Martina de Geus,^a Supriyo Sinha,^{a‡} and Andrew Homyk^a

^a Verily Life Sciences LLC, 249 E. Grand Avenue, South San Francisco, CA 94080 USA

* Tel: +1 415-736-5695 (office); E-mail: saurabhv@verily.com

‡ Current Address: Twenty/Twenty Therapeutics, 259 East Grand Avenue South San Francisco, CA 94080 USA

S1 Materials

We use Novec HFE-7500 (3M, Minneapolis, MN) as the inert fluorinated oil. For surfactant, we added Evagreen oil (Bio-Rad, Hercules, CA) to HFE-7500 in a 1:5 ratio. The aqueous fluid was buffer or distilled water. PBS was used with beads, RPMI media for tests with mammalian cells. Media was obtained from ThermoFisher (Waltham, MA); microbeads were obtained from Spherotech Inc (Lake Forest, IL) and Bangslabs (Fishers, IN).

PDMS devices were made using the recommended 1:10 ratio of Sylgard, and the material was obtained from WPI (Sarasota, FL). Topaz COC pellets for injection molding and making films were obtained from PolyPlastics USA (Farmington Hills, MI). All other chemicals were obtained from Sigma Aldrich (St Louis, MO).

Tubing and other fluidic components were obtained from IDEXX Inc (WestBrook, ME). Syringe pumps were obtained from KDS Scientific (Holliston, MA).

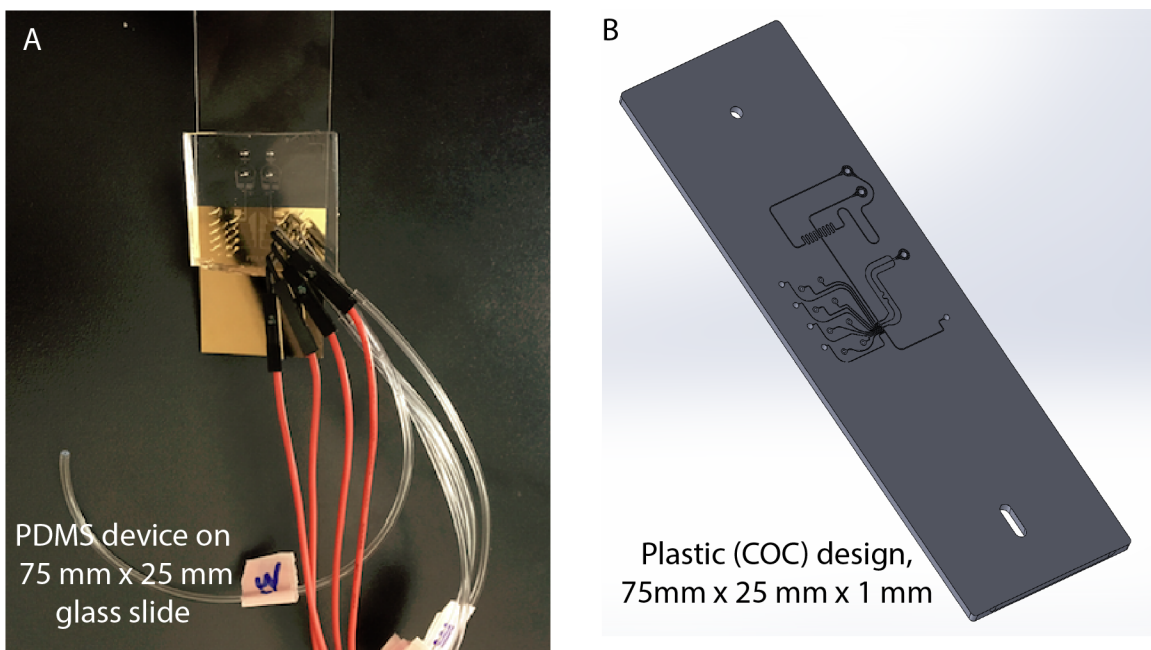


Figure S1 (A) A complete PDMS 4-sort device with some of the tubes and wires attached. Bulk PDMS chip is bonded to a glass slide, coated with PDMS membrane (insulator) and half coated with gold (ground). (B) A CAD model of the 4-sort COC plastic device. The device dimensions are 75 mm x 25 mm x 1 mm. A thin COC membrane is bonded to this device to serve as top cover.

S2 Device Fabrication

Designs were made in AutoCAD/KLayout (for PDMS) and Solidworks (for COC).

S2.1 PDMS Devices: Softlithography

PDMS devices were made by photolithography with SU8 3050/3035 photoresist (Kayaku Advanced Materials, Japan - formerly Microchem Inc) followed by soft lithography. Holes were punched with a coring punch (Syneo Accu Punch MP10). The devices were bonded using oxygen plasma treatment (Harrick Plasma Cleaner PDL-001-HP) to gold coated glass slides covered with a spin coated insulating layer of PDMS (2600 rpm for 1 min). Gold was coated on half the glass slide, covering only the electrode region, while leaving the optical detection region transparent.

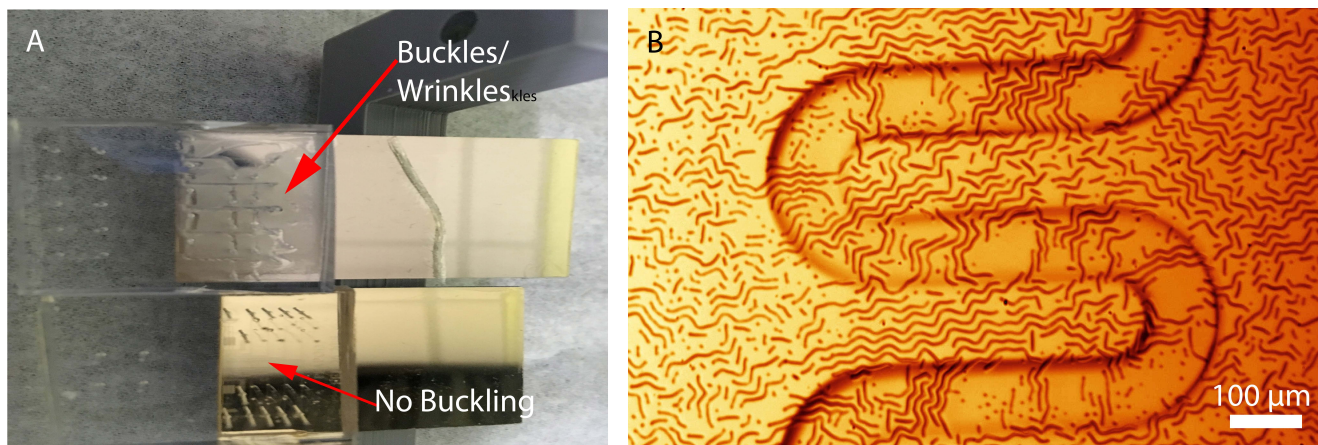


Figure S2 PDMS wrinkles on gold (A) A comparison between PDMS devices bonded to a gold coated slide: one without a glass coating on top, and another with the coating. (B) A PDMS serpentine channel 100 micron wide (part of a 2-sort device) that develops wrinkled features when a film of glass was not deposited on the gold (false color).

A small layer of silicon dioxide was deposited on top of the gold in order to improve bonding to PDMS. If we did not deposit this layer we found a wrinkling/buckling effect, and eventual delamination of the device (Fig. S2). The deposition scheme used was a layer of chromium (5 nm) to improve gold adhesion followed by gold (30 nm), and a thin layer of glass (20 nm). The device channels were not treated, but used a few days after bonding, when the hydrophilicity had worn off.

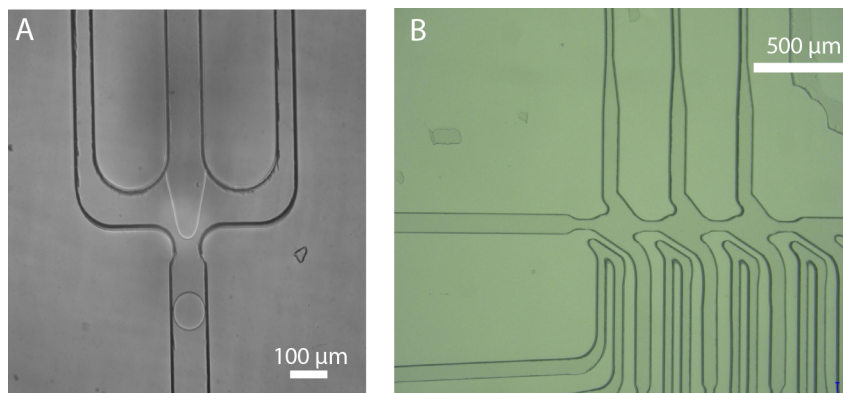


Figure S3 Plastic devices (A) Droplets being made at the nozzle of a plastic COC device. A 50 micron COC film serves as top cover. (B) A view of the sorting section. The electrodes are 35 micron at their closest approach to the flow channels in this picture. The main channel is 100 micron at its widest.

S2.2 COC Devices: Injection Molding

Plastic COC devices were made in two ways: 1) externally, to our specification by microfluidics Chipshop (Jena, Germany). An off-the-shelf 50 micron COC membrane was bonded to create a cover for these devices. 2) internally, Verily Life Science's machining/injection molding lab made devices for us. The process involved precision machining an aluminum mold followed by injection molding. We used Topaz 5013L for the bulk plastic chip, and made cover membranes by dissolving COC Topaz 8007X in sec-butyl benzene at a 30% v/w concentration, and spin coating a film at 1000 rpm on a glass slide. The film was dried on a hot-plate at 100 C for a few hours. Following this, the films were released, cut, and bonded to the injection molded bulk COC chip. A hot press (Carver 4386) was used to lightly adhere the film, with a final bonding step in an oven.

We used a laser cut brass shadow mask or a photolithographic brass shadow mask (Fotofab Inc, Chicago, IL) to selectively coat gold using e-beam evaporation, both for the gold ground film on the membrane side and the connections to the ionic liquid electrodes on the other side.

These devices are comparable in performance to PDMS devices, with the exception that high power blue/UV lasers can cause holes to develop in the thin membrane, possibly due to a small amount of energy absorption by the plastic at those wavelengths.

S3 Opto-electronics and Software

The optical detectors include PMTs (photomultiplier tubes) to measure fluorescence (Hamamatsu, Japan), and SiAPD (silicon avalanche photodiode) detectors (Thorlabs) to measure scattered light. Two cameras above and below the chip are used for imaging and alignment (Point Gray Grasshopper3 and Phantom Veo 640). One camera focuses on the sorting region using illumination provided by an infra-red LED (light emitting diode), reflecting off the ground gold film and illuminating the chip. The other camera is focused on the optical detection region.

The electronics consist of three systems: analog input, digital processing, and analog output. The analog input system is a series of custom PCBAs (printed circuit board assembly) which condition and filter the signal from the optical detectors to allow for digitization of the signal. A two stage amplification system consisting of a transimpedance amplifier and a differential amplifier convert the current output of the detectors into the appropriate voltage for the ADCs (analog to digital converter).

The gain of the PMTs is digitally adjustable via a custom PCBA with a multi-channel high resolution DAC (digital to analog converter). The fluorescence signal is digitized by analog to digital converters (ADCs) integrated on a microprocessor (Texas Instruments, Dallas, TX). The ADC's digitize the signal at 1 MSPS (million samples per second) and 16 bits. The microprocessor's integrated voltage comparators with digitally adjustable thresholds are used to initiate digitization and timestamp events. The analog output system has individually controllable outputs for each sort junction present on the microfluidic chip. A custom PCBA takes a digital logic input, and when the logic level of the input is high, the output is a high voltage AC signal which is connected to the electrodes on the chip. The power supply for the high voltage system consists of two PS300 DC high voltage power supplies (Stanford Research Systems, Sunnyvale, CA), and a 33500B frequency generator (Agilent/ Keysight, Santa Rosa, CA) that supplies the clock signal.

S3.1 Control Firmware

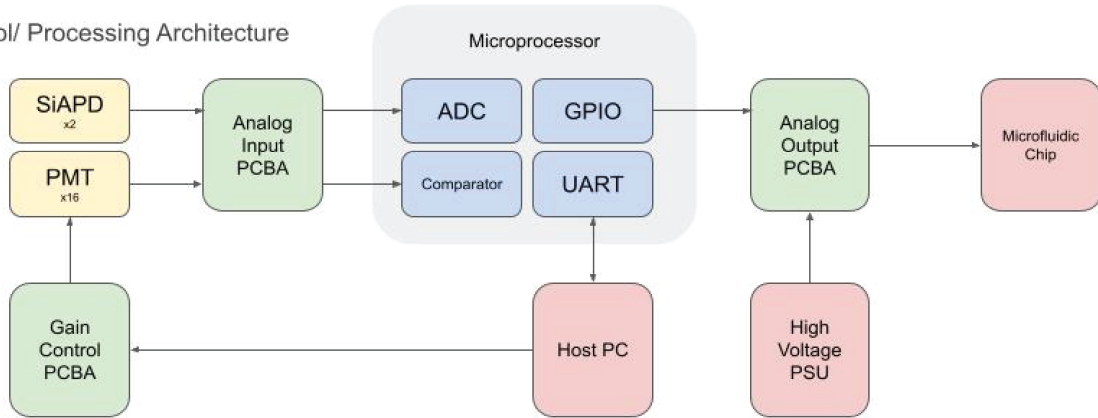
The ADCs constantly digitize the signal from the fluorescent detectors into the microprocessor RAM (random access memory) using a ping-pong buffer scheme and the processor's DMA (direct memory access) functionality to minimize processor overhead. When the forward scatter detector signal crosses the threshold of a voltage comparator, the digitization is programmed to retain a fixed number of pre-trigger samples in memory, and to fill the remainder of a fixed size sample buffer. A peak detection algorithm performs a background subtraction and determines if any fluorescent signal was detected for each excitation/emission pair. The spatial separation of the lasers is used to demultiplex the signals originating from different excitation lasers. The peak height, peak width, and peak area are calculated for all events. The statistics from a single droplet are compared to user provided parameters (i.e. gates) and a sort/no sort determination is made. If a droplet is to be sorted, the microprocessor determines the latency until the droplet is in the correct sorting zone on the chip for the appropriate junction. At the correct time, a scheduling algorithm activates a digital output signal which is fed into the analog output system.

S3.2 User Interface

The microprocessor sends data to and receives commands from a host PC over a serial interface. A user interface displays data and operational metrics received from the microprocessor. Users can create traditional flow cytometry plots and gates to control the sorting behavior of the system, as well as adjust thresholds and timing parameters. Datasets can be stored on the PC to be viewed later.

A

Control/ Processing Architecture



B

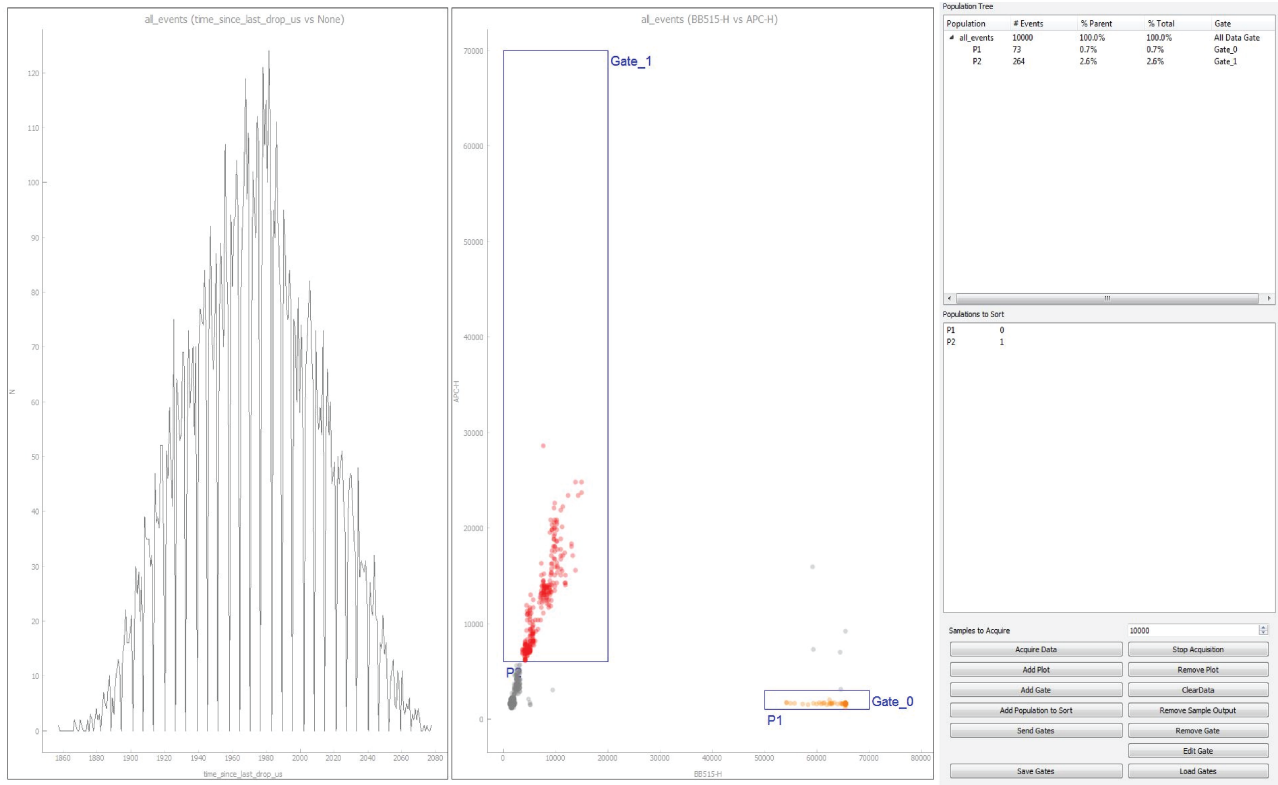


Figure S4 Control system and software interface (A) The overall system architecture. Analog signals from detectors are converted into digital signals. The scatter signal from a drop is used as a trigger to start acquisition. The fluorescence/scatter signal received can be used to decide whether to sort a drop into a particular output. Abbreviations - SiAPD: silicon avalanche photodiode, PMT: photomultiplier tube, PCBA: printed circuit board assembly, ADC: analog to digital converter, PC: personal computer, GPIO: general purpose input output, UART: universal asynchronous receiver transmitter, PSU: power supply unit. (B) A screen grab snapshot of the software's graphical interface which enables setting the timing parameters, and selecting the gates for sorting into a particular sort channel.

S4 Electrical Circuit Analogy

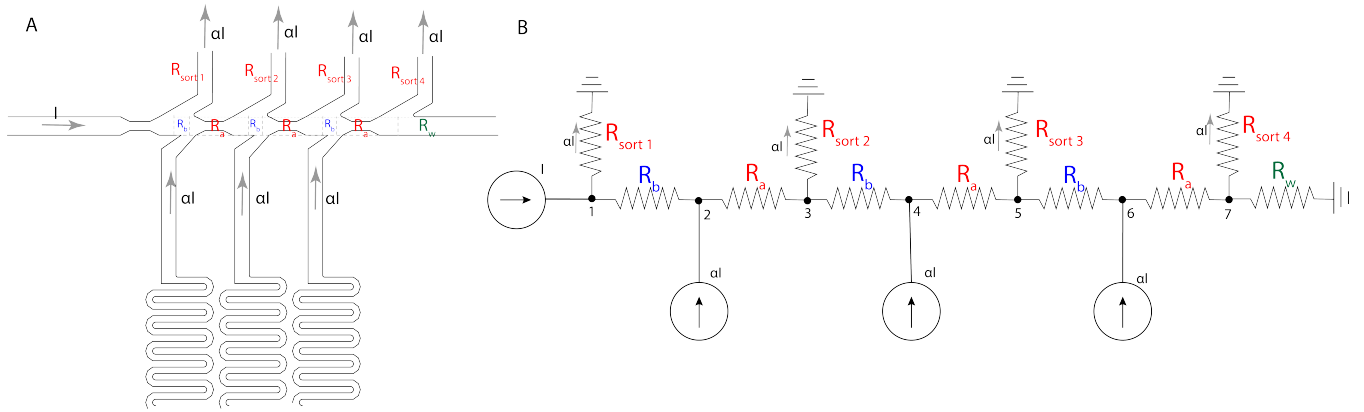


Figure S5 (A) The fluidic system (here a 4-sort device) can be modelled as a simplified electrical circuit, where the current I corresponds to the flow rate, voltage V to the pressure, and resistance R to the fluidic resistance of the flow channels. The relevant fluidic resistances have been labeled. Some parts are modeled as current sources. (B) The corresponding electrical circuit. We assume that the side oil channel have high resistance and can be modelled as current sources. Similarly, the main flow can be modeled as a current source. The sort channels are supposed to divert α fraction of the main flow, which in turn is resupplied by the side oil line.

We can make an electrical circuit analogy to our fluidic design, shown in Figure S5 for a design with 4 sort junctions. The assumptions are that flows are modelled as low Reynolds number (laminar) flows, and therefore the equivalent of Ohm's law ($V = IR$) holds for fluidics. The circuit model approximates a continuous system to a lumped element system and ignores any multiphase flow complications. The current I corresponds to the flow rate, voltage V to the pressure, and resistance R to the fluidic resistance. Like electrical resistance, the fluidic resistance of a channel with rectangular cross section is proportional to its length, and is given by:

$$\frac{12\eta L}{wh^3 \left(1 - \frac{h}{w} \left(\frac{192}{\pi^5} \sum_{n=1,3,5,\dots}^{\infty} \frac{1}{n^5} \tanh\left(\frac{n\pi w}{2h}\right) \right) \right)} \quad (1)$$

where h is the height, w the width, L the length, and η is the viscosity.

To complete our electrical circuit analogy we assume, by design, that the side oil channels have high fluidic resistance compared to other fluidic resistances in the fluidic circuit, and because we are using syringe pumps to push fluids, we can model side oil channels as ideal current sources. In the design, this is achieved using narrow width, serpentine (i.e long) channels. Similarly the main flow is also modelled as an ideal current source.

From the electrical circuit, a nodal analysis on the nodes numbered 1 to 7 as shown in Fig S5B, gives the matrix equation:

$$\begin{bmatrix} \frac{1}{R_b} + \frac{1}{R_{sort1}} & -\frac{1}{R_b} & 0 & 0 & 0 & 0 & 0 \\ -\frac{1}{R_b} & \frac{1}{R_b} + \frac{1}{R_a} & -\frac{1}{R_a} & 0 & 0 & 0 & 0 \\ 0 & -\frac{1}{R_a} & \frac{1}{R_b} + \frac{1}{R_{sort2}} + \frac{1}{R_a} & -\frac{1}{R_b} & 0 & 0 & 0 \\ 0 & 0 & -\frac{1}{R_b} & \frac{1}{R_b} + \frac{1}{R_a} & -\frac{1}{R_a} & 0 & 0 \\ 0 & 0 & 0 & -\frac{1}{R_a} & \frac{1}{R_b} + \frac{1}{R_{sort3}} + \frac{1}{R_a} & -\frac{1}{R_b} & 0 \\ 0 & 0 & 0 & 0 & -\frac{1}{R_b} & \frac{1}{R_a} + \frac{1}{R_b} & -\frac{1}{R_a} \\ 0 & 0 & 0 & 0 & 0 & -\frac{1}{R_a} & \frac{1}{R_a} + \frac{1}{R_w} + \frac{1}{R_{sort4}} \end{bmatrix} \begin{bmatrix} V_1 \\ V_2 \\ V_3 \\ V_4 \\ V_5 \\ V_6 \\ V_7 \end{bmatrix} = \begin{bmatrix} I \\ \alpha I \\ 0 \\ \alpha I \\ 0 \\ \alpha I \\ 0 \end{bmatrix} \quad (2)$$

Resistances R_a , R_b and R_w are known from the chosen design. We pick α to be 0.3. The value of current is just a scale factor that can be taken to be one. These equations can be solved for the voltages V_1 to V_7 , and a multidimensional minimization routine can be used to compute for the sort resistances (R_{sort1} , R_{sort2} , R_{sort3} , and R_{sort4}) that minimizes:

$$\left(\alpha - \frac{V_1 R_{sort1}}{I} \right)^2 + \left(\alpha - \frac{V_3 R_{sort2}}{I} \right)^2 + \left(\alpha - \frac{V_5 R_{sort3}}{I} \right)^2 + \left(\alpha - \frac{V_7 R_{sort4}}{I} \right)^2 \quad (3)$$

This quantity ensures we obtain sort resistances that divert fraction $\alpha = 0.3$ of the main flow at each sort junction as closely as possible. The fluidic resistances obtained are converted into appropriate channel dimensions using Equation 1.

While this procedure is a simple approximation, we find it works well for our design and operating conditions, and can be extended to designs with more sort junctions. If changes in design or operating conditions make the approximations untenable, or if more accuracy is desired, then a more sophisticated calculation using fluidic simulations, possibly incorporating multiphase flows, is possible with computational fluidic dynamics software like Ansys Fluent.

S5 Additional Images

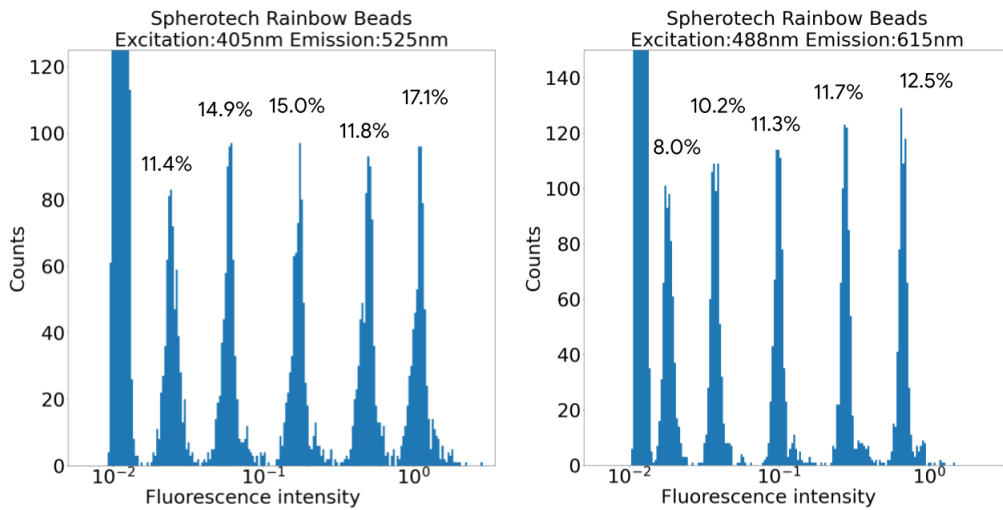


Figure S6 We are able to measure fluorescence to a 3 log dynamic range in many channels. The figure shows fluorescence in two channels (emission 405 nm, excitation 525 nm; excitation 488 nm, emission 615 nm) collected from a set of rainbow beads with 5 levels of fluorescence inside drops. CV (coefficient of variation) values are labelled for each peak. Empty drops cause the wall at the lowest fluorescence intensity and sets the floor on system noise. The drops are flowing through a channel of 30 micron height and 50 micron width.

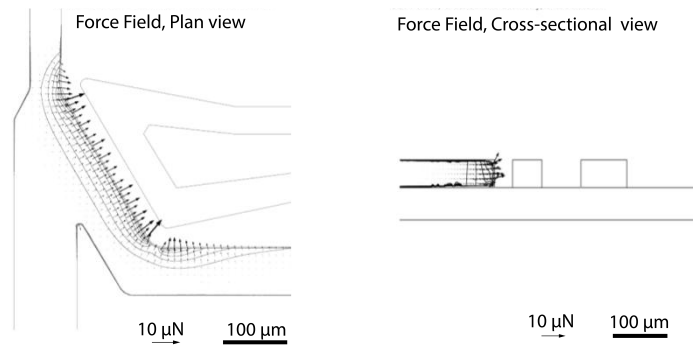


Figure S7 Simulation of the dielectrophoretic sorting force shown in top and side cross-sectional view. The electrode geometry consists of an ionic liquid-filled active electrode and a ground film electrode, separated by a thin insulating film. The force is directed sideways and in the plane of the channel, a consequence of having a ground plane. In general, the magnitude will scale with driving voltage, particle volume and permittivity. Regions near channel boundaries would not be reachable by larger particles, and are shown here only to illustrate uniformity and spatial dependence.

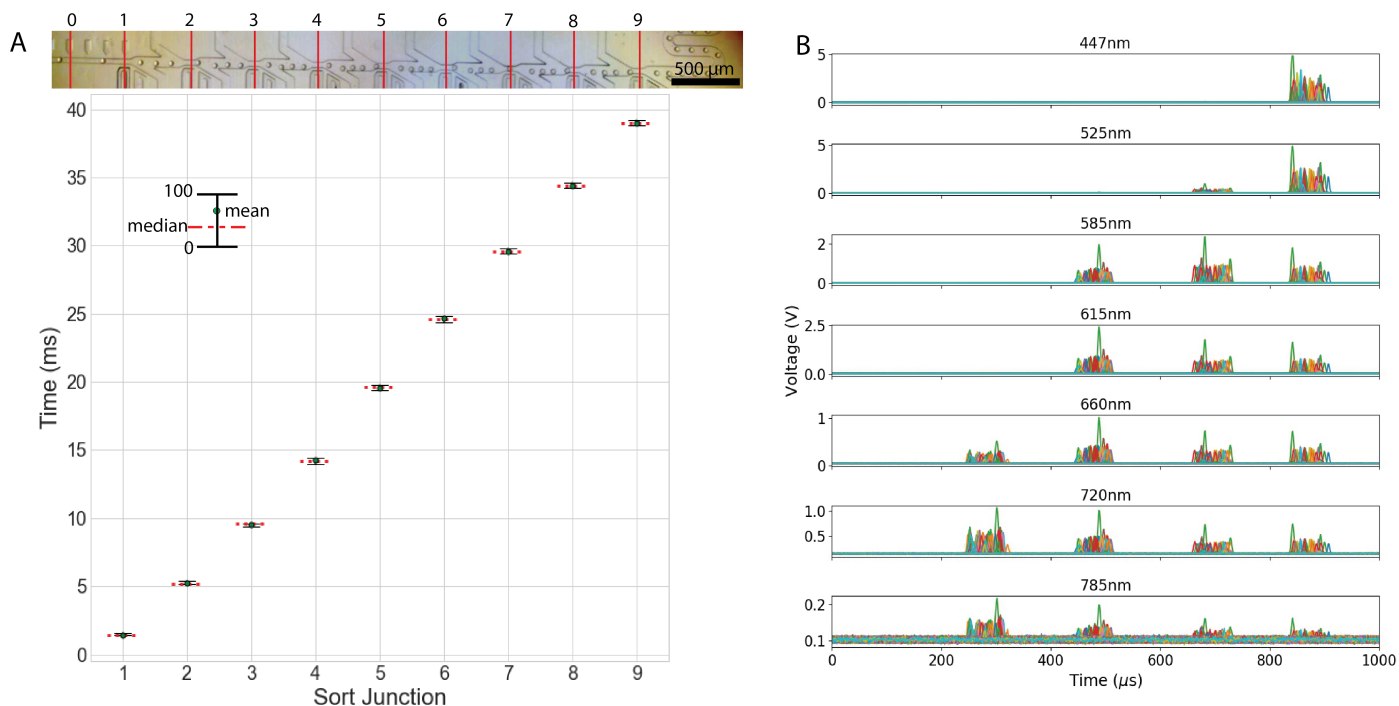


Figure S8 Timing drops (A) Video of drops flowing through a 9-sort device was used to compute the time of arrival of 800 drops at sort junctions. Every timing for all time points for each junction lies within a 1 ms window, with standard deviation less than 0.5 ms for every junction. (B) Fluorescence readout from rainbow beads in drops as they move across the laser line in 7 channels. The beads can be located anywhere in the drop and this results in dispersion; however, fluorescence due to each laser can be separated out in time. We are using scatter from the drop as it crosses the first laser to trigger the start of an event and collect fluorescence. We also collect a few pre-trigger signals.

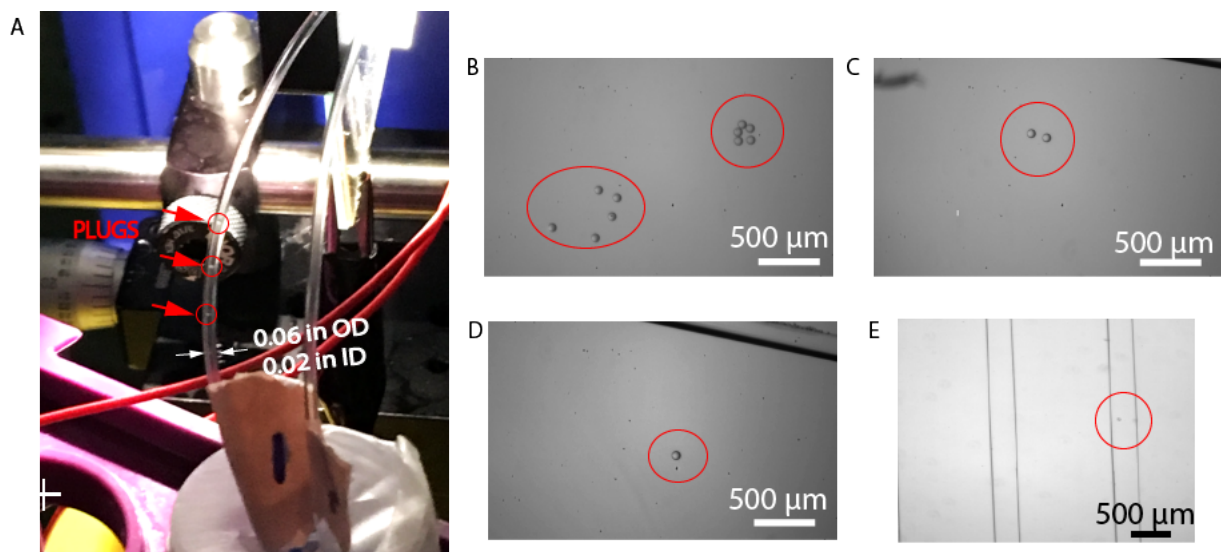


Figure S9 Effect of tubing on sorted drops (A) Sorted drops coalesce to form plugs moving at unpredictable rates in a large bore tubing (500 micron here). The plugs can be observed as the tube is transparent. (B)-(D) Narrow bore tubing prevents coalescence. Here 125 micron inner bore was used. 5, 2 or 1 drops were sorted for every 1000 drops, with a droplet rate of 350/s. If we collect fluid from the sort outlet, we see a pulse of droplets every 3-4 seconds. The drops are <100 pl, and the oil collected is less than 5 μl. (E) We connected the two sort outlets of a 2-sort to another chip with two long channels, using narrow bore tubing. The channels were imaged on a microscope. Single drops were sorted into one of the sort junctions, and then observed to flow by several seconds later in the channel.

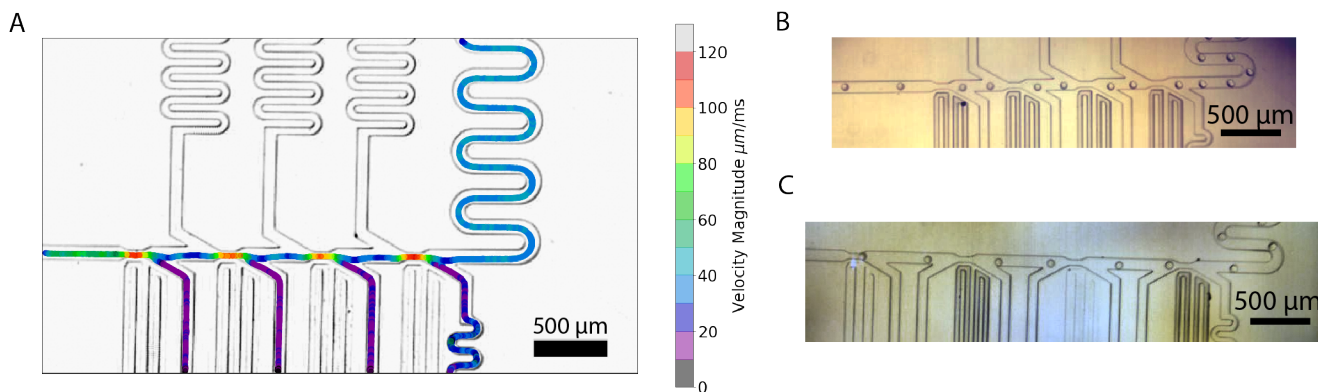


Figure S10 Drops flowing through sorting junctions (A) Using videos, the path and velocity of 200 drops were overlaid on a 4-sort design. Drops were being sorted in 1234W1234W1234W... pattern where the number is the sort junction and W is waste. Notice the similarity of flow at each sorting junction (B),(C) The side oil supply may be arranged to be on the same side or the opposite side to the sort channels. The opposite side configuration is more compact compared to the same side design, but either may be used.

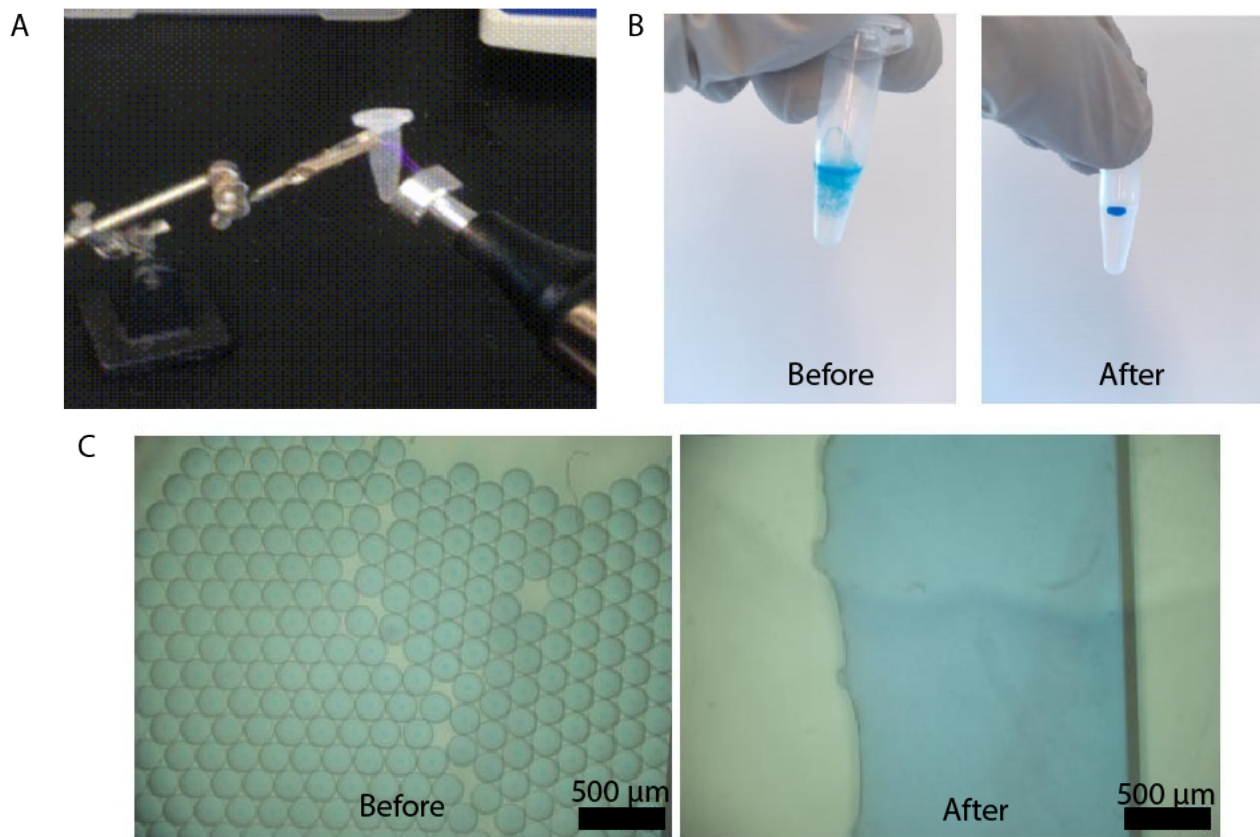


Figure S11 Emulsion breaking using a corona discharge machine. (A) Corona discharge wand brought close to a centrifuge tube for emulsion breaking. (B) Before and after image of an emulsion on application of corona discharge. (C) Before and after photos of the emulsion breaking in a plastic haemocytometer.

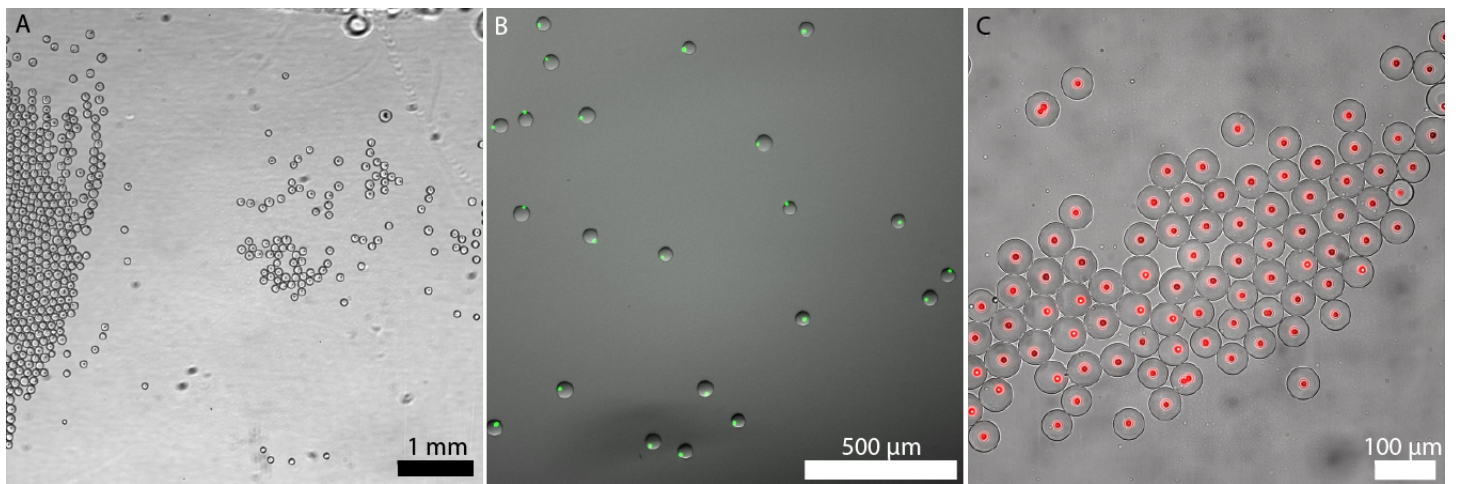


Figure S12 Sorting fluorescent beads (A) Drops from a sort experiment collected in a haemocytometer. (B) Fluorescence (Alexa 447), pseudo color, overlaid on a brightfield image. In this case, the sorting was done on a 4-sort plastic chip. (C) Sorted drops with Alexa 647 fluorescent beads (pseudo color), in this case collected from a 4-sort PDMS device.

S6 Videos

Video S1

Droplets sorting in a 11223344WW pattern, where the number is the sort output and W is waste. The approximate droplet velocity was calculated from video frames overlaid as an arrow, with some jitter. Droplet rate is approximately 90 Hz. The camera frame rate was 2500 frames per second. Video slowed 100x.

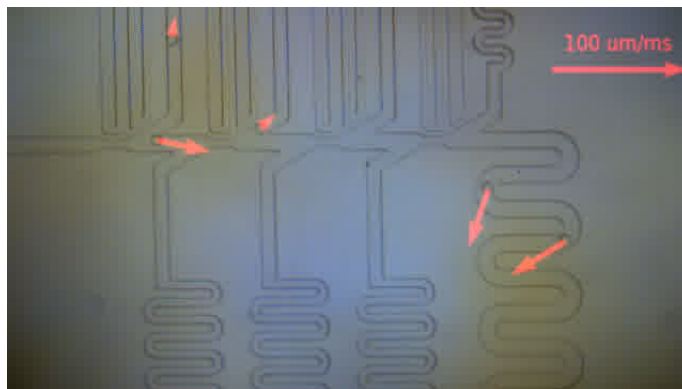


Figure S13 Snapshot of Video S1

Video S2

17 junction sorting with two drops being sorted in junction 3 and 15. Drops flowing at approximately 230 per second. Original video taken at 2500 frames per second. Video slowed 100x.



Figure S14 Snapshot of Video S2

Video S3

Drops being sorted such that 1 in 3 drops go into each of the 8 sort outputs. Droplet rate is 660 Hz. Original video taken at 10000 frames per second. Video slowed 2000x.

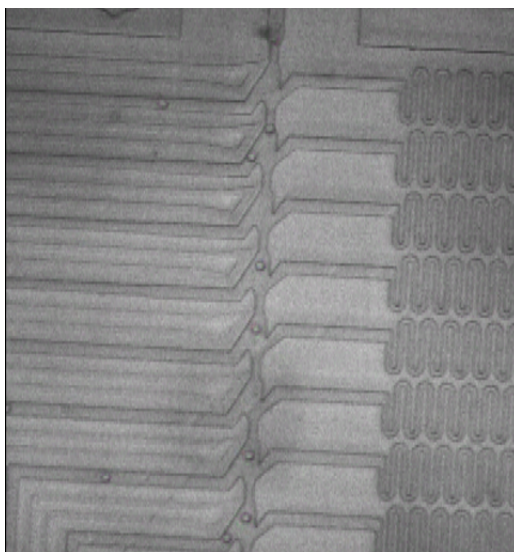


Figure S15 Snapshot of Video S13

Video S4

Cells being sorted into two sort outlets based on fluorescence labelling with FITC and Pe-Cy5 dyes. Original video taken at 10000 frames per second. Video slowed 1000x.

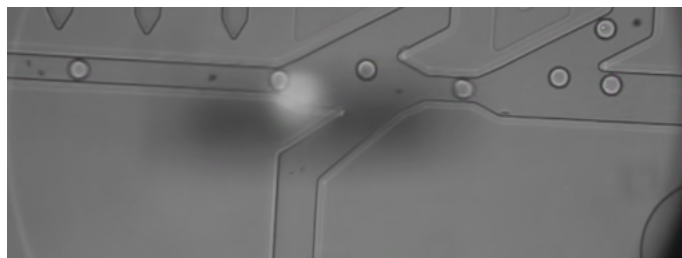


Figure S16 Snapshot of Video S4

Video S5

Droplet sorting in a COC plastic 4-sort chip. The background has been subtracted to make the droplets more visible. Drops are being sorted in 1x2x3x4x order where x is a no-sort and 1,2,3,4 are the 4 sort outlets. Drop frequency was about 700 Hz. Camera frame rate is 10000 frames per second. Video slowed 1000x.

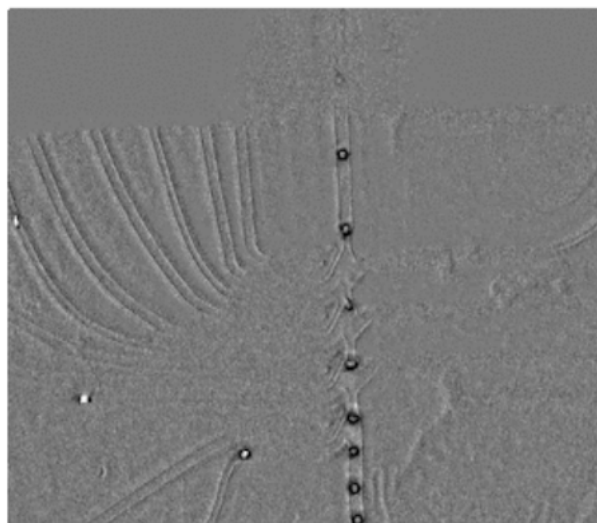


Figure S17 Snapshot of Video S5